The Elimination of Toluenediamine from Aqueous Solution by Reverse Osmosis

Shokri, Aref*[+]

Department of Chemistry, Payame Noor University (PNU), Tehran, Iran

ABSTRACT: *Toluene diamine (TDA) is a main carcinogenic aromatic pollutant in some industrial wastewater. In this study, the reverse osmosis with DSS-HR98PP as the membrane was employed for the removal of TDA in an aqueous environment. The Box–Behnken Design (BBD) of the experiment was used to consider the effect of operational variables such as pressure, pH and the feed volumetric flow rate on the rejection efficiency of TDA. The ANOVA (Analysis of variance) exhibited a reasonable prediction second-order regression model and a high determination coefficient values (R^2 = 99.57, R^2_{adj} = 98.81 and R^2_{pred} = 93.20). The optimum conditions predicted by the model were as follows: the volumetric flow rate of feed at 6 $\times$ 10^{-5} m^3/m^2s, pH at 6.8, and pressure at 45 $\times$ 10^{-5} N/m^2. The predicted optimum response was 98.2%. The results showed that at the optimum conditions obtained for rejection, the permeate flux and actual rejection efficiency were 44.3 $\times 10^4$ m^3/m^2s, and 96.9%, respectively.*

KEYWORDS *Rejection efficiency; Toluene diamine; Reverse osmosis; Box–Behnken design; permeate flux.*

INTRODUCTION

One of the main aromatic pollutants in Karoon petrochemical company in Iran is 2, 4-Toluene diamine (TDA). It is a main carcinogenic raw material for the production of toluene diisocyanate (TDI), dye corrosion inhibitors, rubber antioxidants and polyurethane foams [1]. These pollutants can be transported to surface water by the release of wastewater from industrial plants. The solubility of TDA in water is high and it can penetrate through soil causing the groundwater to be contaminated [2–3]. Aromatic amines are mutagenic in microorganisms and mammalian cells, and have been reported to be cancer-causing in rodents. Therefore the remediation of wastewater containing aromatic pollutants is essential. There are many methods to remediate different kinds of pollutants [4–5]. The shortages of freshwater and developed membrane performance have caused the growing use of Reverse Osmosis (RO) for the creation of potable water and the reuse of industrial wastewater. The common commercial RO plants are employed for the desalination of seawater and salty water; although the number of RO plants handling municipal and industrial wastewater for recycling is still restricted [6].

Membrane systems are appreciated methods for the wastewater because of the many profits such as low power weakening, high quality of water and low area required [7]. The reverse osmosis (RO) is one of the membranes

* *To whom correspondence should be addressed.*
+ *E-mail aref.shokri3@gmail.com*
1021-9986/2019/5/121-128 8/$/5.08

technologies that can remove the organic pollutants [8]. RO processes can considerably drop the volume of waste streams and the pollutions are concentrated into a small volume compared to the total waste size. Both organic and inorganic pollutants can be eliminated directly by RO membrane processes. Extra advantages of RO process are energy-saving, simple design and easy to work, in comparison with ordinary methods. But fouling, scaling, and concentration polarization can decline the efficiency of the RO method [9–10]. The RO system cannot degrade the toxic pollutants, but it can transfer the pollutants from one phase to another and this issue is one of the main restrictions of RO methods, but in the separation of pollutants and reusing them it can be considered as a useful technique for wastewater treatment.

Several processes for the removal of TDA from wastewater have been studied, including Persulfate oxidation [11] and UV/H_2O_2 processes [12]. The main purpose of this study is to apply the Box-Behnken design of an experiment for the optimization of operational variables such as pressure, pH and the volumetric the flow rate of feed on the rejection performance of the TDA as a response function.

EXPERIMENTAL SECTION

Materials

TDA (98%) was purchased from Sigma-Aldrich, China. TDA stock solution (100 mg/L) was synthesized with distilled water. All chemicals were of reagent grade and used without further purification. The features of TDA were shown in Table 1. The pK_a shows the acid dissociation constant at which the organic molecule loses a hydrogen atom and becomes negatively charged and log (K_{ow}) exhibits the hydrophobicity of the organic molecule. A thin film composite polymeric polyamide membrane (DSS-HR98PP) produced by Alfa Laval (Manufacturer Dow Chemical) was employed. The analytical grade reagents used in this research were sodium hydroxide and sulphuric acid, supplied from Merck. Distilled water was used during this study.

Experimental setup

The RO experiments were performed using the pilot plant organized in Fig. 1. The feed tank with a capacity of 10 L is a closes stainless steel container. The setup was equipped with an RO membrane, diaphragm pump (HEADON model HF-8367) with a maximum flow rate of 10^{-4} m^2/s, membrane module, one diaphragm valve, and pressure gauge. The maximum pressure of the membrane was 55×10^5 N/m^2. The adjusting of the feed flow rate was performed by a flow meter combined with a needle valve on the feed stream. A second globe valve was used for pressure regulation. A pressure gauge was positioned for monitoring the inlet feed pressure.

Methods

A supply tank was filled with dissolving the required amount of TDA in distillate water. The solubility of TDA in water in alkaline pH is more than acidic and neutral medium. The concentration of TDA was fixed at 100 mg/L in all runs. Different pH at 5, 7 and 9 were prepared by adding a dilute solution of sodium hydroxide and sulfuric acid for investigating the influence of pH. The effect of feed flow rate at 2, 4, and 6×10^{-5} m^3/s and the influence of feed pressure at 25, 35 and 45×10^5 N/m^2 was explored. All experiments were performed at 25°C. The feed solution was pumped into the membrane module with the chosen pressure, pH and flow rate. The rejected and permeated streams were spilled back to the feed, tank to keep the feed concentrations practically fixed and so simulate a continuous process in a quasi-stationary state. The samples were taken from permeate and rejected lines after the steady-state condition. The rejection of Solute was calculated as:

$$R = \left(1 - \frac{c_p}{c_f}\right) \times 100 \qquad (1)$$

Where C_F and C_P are the feed and permeate concentration, respectively [13]. The permeate flux (J_p) can be defined as the volume flowing through the membrane per unit area and time (m^3/m^2s). In this project, the feed solution was diluted and the velocity of the feed was high, therefore the concentration polarization and fouling were not important and minor deviations from the ideal mass transfer were occurring. As it is clear from the following equation, the solvent flow (J_w) depends on the hydraulic pressure used across the membrane (ΔP), minus the difference in the osmotic pressures of the solutions on the permeate and feed side of the membrane ($\Delta\pi$).

$$J_w = A_w \left(\Delta P - \Delta\pi\right) \qquad (2)$$

Table 1: Chemical properties of TDA.

Pollutant	Molecular structure	λ_{max}, nm	log (K_w)	pK_a	M_w (g/mol)
Toluene-2, 4-diamine (TDA)	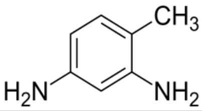	230	0.337	5.58	122.2

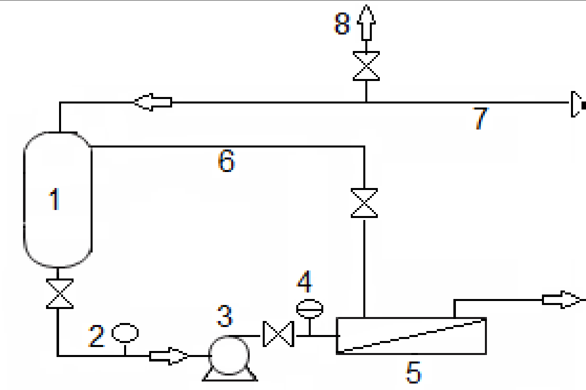

Fig. 1: Schema of the experimental RO pilot plant: (1) Feed tank, (2) Instrumentation Device, (3) Diaphragm pump, (4) Pressure indicator, (5) Membrane module, (6) Reject line, (7) Permeate line, (8) Sampling valve.

Where A_w is the water permeability constant, which can be subjected by the features of the membrane and $\Delta\pi$ signifies the osmotic pressure difference across the active layer of the membrane [14]. The solute flux (J_s) depends on the differences in solute concentration across the membrane.

$$J_s = B_s\left(C_s - C_p\right) \quad (3)$$

The B_s is the solute permeability constant, which depends on the solute composition and
the membrane structure, with the following values:

$$B_s = \frac{K_s D_s}{l} \quad (4)$$

Where K_s is the solute distribution coefficient, D_s is the diffusion coefficient of solute, and l is the membrane width. The permeate concentration can be introduced as $C_p = J_s/J_w$ [15].

The concentration of TDA in the feed and permeate solutions was estimated by UV–Vis spectrophotometer (Agilent, 5453, American) at 230 nm.

RESULTS AND DISCUSSION

The Box-Behnken experimental Design (BBD) was used with three independent variables comprising the pressure (P), the feed volumetric flow rate (Q), and pH. The experimental design method was employed and the rejection efficiency of TDA was nominated as a response to get the optimum conditions. The input variables and their levels in the experiment were presented in Table 2.

Data analysis

The BBD needs fewer runs than all other RSM designs [16]. The ensuing model was fitted with the rejection efficiency (Y) in the arrangement of a polynomial equation (Eq. 5):

$$Y = b_{\circ} + \sum b_i x_i + \sum\sum b_{ij} x_i x_j + \sum\sum b_{ii} x_i^2 + \varepsilon \quad (5)$$

Where ε is the residual term, b_0 is a constant, b_{ij} is the linear interaction effect between the input variables, x_i and x_j (i=1,2 and 3; j= 1,2 and 3) are independent variables, b_i is the slope of the variable, b_{ii} is the second order of input variable (x_i). The ANOVA was employed to explore the significance of each term in the polynomial equation [17]. The MINITAB 17 was used to determine the coefficients of Eq. (5) with RSM. The experimental design composed of 15 tests and the natural values of these variables, the experimental and predicted response values for the rejection efficiency are presented in Table 3. In all runs, the time of process was 60 min.

Table 2: The range and levels of the factors.

variables	Symbol	Range and levels		
		-1	0	+1
Pressure × 10^{-5} N/m^2	P	25	35	45
pH	pH	5	7	9
Volumetric flow rate of feed × 10^{-5} M^3/m^{2}s	Q	2	4	6

Table 3: Experimental design for three independent variables and the response.

Run No.	Manipulated variables				Rejection efficiency, %
	p	pH	Q	Exp.	Pred.
1	35	5	6	81.3	81.00
2	45	7	2	91.0	90.55
3	25	9	4	67.4	68.05
4	25	7	6	90.0	90.45
5	45	9	4	74.0	74.15
6	25	5	4	72.0	71.85
7	35	5	2	72.6	73.70
8	35	7	4	91.6	91.60
9	35	7	4	91.6	91.60
10	25	7	2	84.0	83.05
11	35	7	4	91.6	91.60
12	45	5	4	81.5	80.85
13	45	7	6	97.1	98.05
14	35	9	6	77.0	75.90
15	35	9	2	68.0	68.30

Central Composite Design (CCD) model

This section aimed to find out the optimum condition for maximum rejection efficiency. The stages of the CCD were investigated by many researchers [18–19]. The 3-factors CCD matrix and experimental results obtained for the rejection efficiency are presented in Table 2.

The correctness of the model is illustrated in Fig. 2, which compares the experimental values in contradiction of the predicted responses of the model in rejection of TDA. These results showed a good concurrence between predicted and experimental values. It was observed that the predicted response from the model is in coincidence with the experimental data.

ANOVA tests for the rejection efficiency in RO process

In this research, the effect of three independent variables on the response function was explored by using the BBD and the RSM, to get the optimal conditions. The mathematical relation between the response and three significant variables can be evaluated by a quadratic polynomial equation [20–21]. The equation for the rejection efficiency is proposed through the following equation (Eq. (6)):

$$\text{Rejection efficiency}\,(\%) = -147.2+1.352P+58.81pH+1.76Q-0.01037P^2-4.209pH^2-0.009Q^2-0.0363P.pH+0.0013P.Q+0.019pH.Q \quad (6)$$

Table 4: ANOVA test for quadratic model for the rejection efficiency in RO process.

Sources	DF	SS	MS	F-value	P-value
Model	9	1335.02	148.34	130.12	0.000
Linear	3	280.14	93.38	81.91	0.000
P	1	114.01	114.01	100.00	0.000
pH	1	55.12	55.12	48.36	0.001
Q	1	111.01	111.01	97.37	0.000
Square	3	1052.75	350.92	307.82	0.000
P^2	1	3.97	3.97	3.49	0.121
pH^2	1	1046.77	1046.77	918.22	0.000
Q^2	1	0.01	0.01	0.00	0.949
2-Way Interaction	3	2.13	0.71	0.62	0.631
P.pH	1	2.1	2.1	1.84	0.233
P.Q	1	0.00	0.00	0.00	0.964
pH.Q	1	0.02	0.02	0.02	0.894
Error	5	5.7	1.14		
Lack – of – fit	3	5.7	1.90	*	*
Pure error	2	0.0	0.00		
Total	14	1340.72			
Model Summary	S	R^2	R^2_{adj}	R^2_{pred}	
	1.06771	99.57%	98.81%	93.20%	

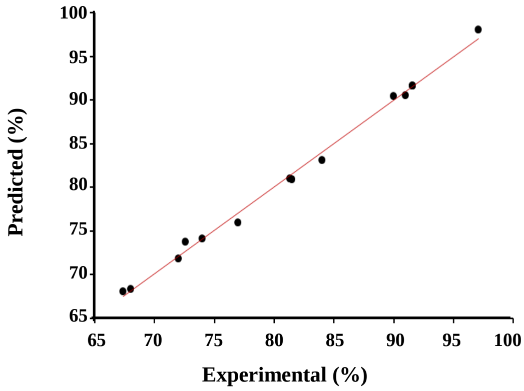

Fig. 2: Comparing the experimental and predicted values for the rejection efficiency in RO process.

The obtained results from the BBD, with residuals for all runs are presented in Table 4. From the above equation (Eq. (6)) it was clear that the pH with higher coefficients (58.81) had the main effect on the rejection efficiency of TDA.

The significance of the coefficients was shown in Table 4. The model terms with a probability value higher than 0.05 were not significant.

Influence of feed pressure on rejection efficiency

The results can be attained as contour plots presentations to study the influence of different variables on the response. Concentration polarization raises the osmotic pressure [22], but in this study, it was not considered because of high feed velocity.

The effect of feed pressure on TDA rejection was tested. As presented in the counterplots (Figs. 3 and 4), the rejection of TDA was increased with an increase in pressure from 25 to 45×10^5 N/m^2. According to the Spiegler–Kedem–Katchalsky model, the driving force for solvent and solute passage is pressure and concentration, respectively. Besides, the solute flux is lower pressure-dependent than water flux. So, the water flux (J_w) is increased directly with pressure and the solute flux is

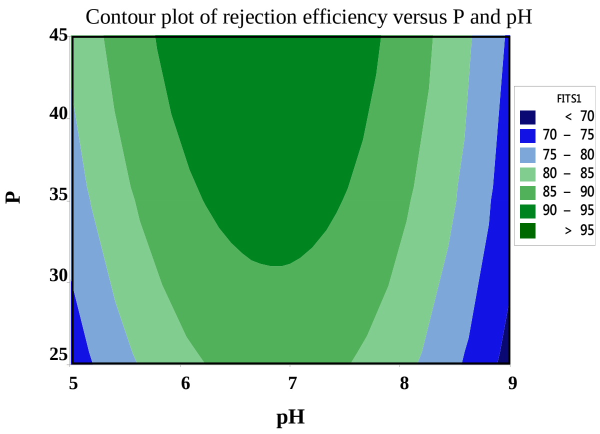

Fig. 3: The contour plot for the rejection efficiency versus: the pressure (P) and pH.

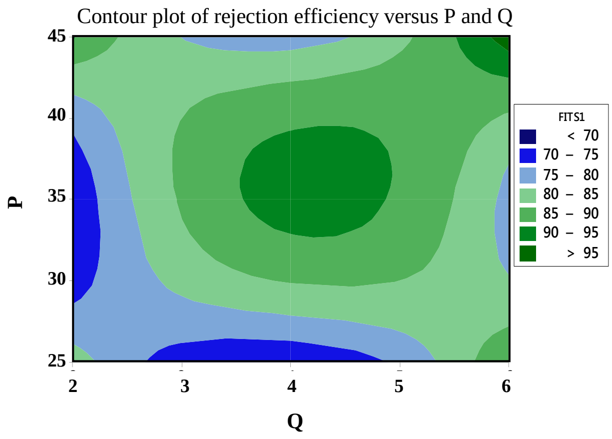

Fig. 4: The contour plot for the rejection efficiency versus: the volumetric flow rate of feed (Q) and pressure (P).

due to concentration differences and water flux. The enhancement in rejection with practical pressure is originated from Eq. (2), where ΔP is the only variable, assuming that the constants A_w and B_s are not relying on on pressure. Higher fluxes achieved from higher membrane pressures lead to lower permeate concentrations, which result in higher rejections. Comparable findings were attained by other authors for the removal of organic contaminants by reverse osmosis membranes and nanofiltration [23].

Influence of feed pH on rejection efficiency

As can be seen from Fig. 3 and 5, the effect of feed pH on rejection efficiency was investigated in the range of 5 to 9. The maximum rejection was achieved at pH of 7 and minimum rejection at pH of 9. The ionization of Polyamide membrane occurred at basic solutions, and the membrane surface negatively charged because of the free carboxylic acid groups in the structure [24]. The change in rejection efficiency versus pH is originated from the presence of ionizable groups in the membrane structure and the net charge of the TDA molecule based on its dissociation equilibrium. The pK_a of TDA is 5.58 and so, at pH values higher than 5.58, the positive structure of TDI will decrease because of the creation of neutral TDI. The improvement in rejection between pH 5 and 7 can be caused by the retention of the remaining TDI cations by the negative carboxylate groups in the membrane. At pH values higher than 7, rejection drops because the amounts of TDI cations decreases significantly and neutral TDI is not taken by the negative charge of the membrane. Similar findings were obtained by other researchers that pK_a and pH values had a very important role in the rejection of Ortho-toluidine and ciprofloxacin, respectively [25–26].

Polyamide membranes have their isoionic point at pH near to 5, and the membrane has a positive charge under this pH and a negative charge over this pH. At a pH of 5, the membrane surface is negatively charged, which leads to an increase of pore size, originated from the electrostatic repulsion between functional groups with the same charge, affecting lower TDI transport. Therefore, the solute flux was slight and the water flux was increased. At a pH of 7–9, the TDI has no net charge, but the membrane will have a negative charge which can increase the water flux, this phenomenon is based on the increase in pore size and a decrease in permeate concentration.

Influence of feed flow rate on rejection efficiency

The effect of feed flow rate on TDI rejection was offered in Figs. 4 and 5. It is clear that the rejection is increased with enhance in the flow rate. By increasing the feed flow rate from 2 to 6×10^{-5} m^3/s, the rejection percent was improved. This result can be described as concentration polarization. The osmotic pressure was reduced in high feed flow rates because of the width of the concentration polarization layer was decreased. According to the Eq. (2), the water flux and the rejection of TDI are increases with decrease the osmotic pressure

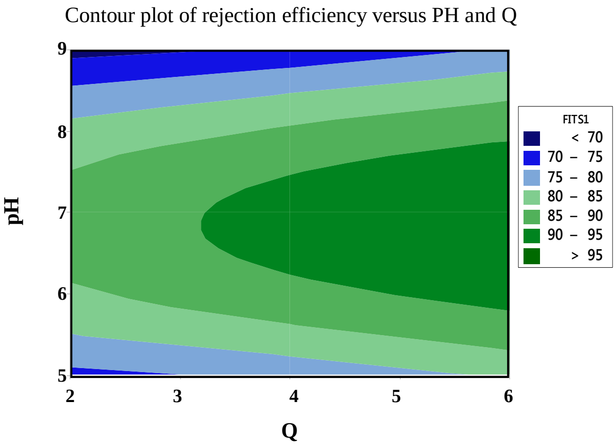

Fig. 5: The contour plot for the rejection efficiency versus The volumetric flow rate of feed (Q) and pH.

difference. The maximum rejection was obtained at 6×10^{-5} m^3/s feed flow rate.

The optimum conditions predicted by the model were as follows: the volumetric flow rate of feed at 6×10^5 (m^3/m^2s), pH at 6.8, and pressure at 45×10^5 (N/m^2). The rejection efficiency proposed by the software was 98.2% in the predicted optimum conditions. The experiment was repeated once again at the predicted optimum condition and the rejection efficiency was 96.9%. In the achieved optimum condition for maximum rejection efficiency, the amount of permeate was obtained at 44.3×10^4 ($m^3/m^2.s$).

CONCLUSIONS

In this project, the Box-Behnken design of the experiment was used for the rejection of Toluenediamine in aqueous solution by RO process.

The effect of operational variables such as pressure, pH and the volumetric flow rate of feed on the rejection efficiency was investigated. The ANOVA tests were performed to find out the importance of independent variables on the response function. The optimum conditions predicted by the model were the volumetric flow rate of feed at 6×10^{-5} ($m^3/m^2.s$), pH at 6.8, and pressure at 45×10^5 (N/m^2). The ANOVA presented a satisfactory prediction second-order regression model and a high determination coefficient values (R^2 = 99.57, R^2_{adj} = 98.81 and R^2_{pred} = 93.20). The counterplots were used to study the role of each factor, as well as their interactions on the rejection efficiency. The rejection percentage was improved with the increase in the volumetric flow rate of the feed and pressure. The observed changes in TDI rejection with pH are originated from the charge of ionizable groups in the membrane structure and to the net charge of TDI molecules.

The results showed that at the optimum conditions obtained for rejection and after 60 min of process the permeate flux and actual rejection efficiency were 44.3×10^4 $m^3/m^2.s$ and 96.9%, respectively. Perhaps the influence of variables on rejection efficiency and the amount of permeate was not the same as to each other, therefore, optimization of variables in permeation efficiency should be performed in future works.

Acknowledgments

The author wishes to thank the HSE department of the national petrochemical company of Iran for scientific guidance.

Received : Apr. 28, 2018 ; Accepted : Jul. 30, 2018

REFERENCES

[1] Shanmugam A., Subrahmanyam S., Tarakad S.V., Kodandapani N., Stanly D.f., 2,4-Toluene Diamines—Their Carcinogenicity, Biodegradation, Analytical Techniques and an Approach towards Development of Biosensors, *Analytical Sciences*, **17**: 1369–1374(2001).

[2] Schupp T., Modeling Formation and Distribution of Toluene-2, 4-diamine (TDA) After Spillage of Toluene-2, 4- diisocyanate (TDI) Into a River, *J. Hazard. Mater.*, **252-253**: 70–76(2013).

[3] Oh S.Y., Cha D.K., Chiu P.C., Graphite-Mediated Reduction of 2, 4-dinitrotoluene with Elemental Iron, *Environ. Sci. Technol.*, **36:**2178–2184 (2002).

[4] Shokri A., Application of Electrocoagulation Process for the Removal of Acid Orange 5 in Synthetic Wastewater, *Iran. J. Chem. Chem. Eng. (IJCCE)*, **38**(2): 113-119. (2018).

[5] Zatloukalova K., Obalova L., Koci K., Photo Catalytic Degradation of Endocrine Disruptor Compounds in Water over Immobilized TiO_2 Photo Catalysts, *Iran. J. Chem. Chem. Eng. (IJCCE)*, **36**: 29–38(2017).

[6] Yangali-Quintanilla V., Maeng S. K., Fujioka T., Kennedy M., Li Z., Amy G., Nano Filtration vs. Reverse Osmosis for the Removal of Emerging Organic Contaminants in Water Reuse, *Desal. Water Treat.*, **34**: 50–56(2011).

[7] Kargari A., Khazaali F., Effect of Operating Parameters on 2-Chlorophenol Removal from Wastewaters by a Low-Pressure Reverse Osmosis System, *Desal. Water Treat.*, **55**: 114–124 (2015).

[8] Alturki A.A., Tadkaew N., McDonald J.A., Khan S.J., Price W.E., Nghiem L.D., Combining MBR and NF/RO Membrane Filtration for the Removal of Trace Organics in Indirect Potable Water Reuse Applications, *Membr. Sci.*, **365**: 206–215(2010).

[9] Ravanchi M.T., Kaghazchi T., Kargari A., Application of Membrane Separation Processes in Petrochemical Industry: A Review. *Desalination*, **235**: 199–244 (2009).

[10] Pena N., Gallego S., Del Vigo F., Chesters S.P., Evaluating Impact of Fouling on Reverse Osmosis Membranes Performance, *Desalin. Water Treat.*, **51**: 958–968 (2009).

[11] Jiang Y.H., Zhang J.B., Xi B.D., An D., Yang Y., Li M.X., Degradation of Toluene-2,4-Diamine by Persulphate: Kinetics, Intermediates and Degradation Pathway, *Environ. Technol.*, **36**: 1441–7(2015).

[12] Hosseini J., Shokri A., Employing UV/H_2O_2 Process for Degradation of 2,4-Diaminotoluene in Synthetic Wastewater, *Arch. Hyg. Sci.*, **6**(2): 121–127 (2017).

[13] Bodalo A., Gomez J.L., Gomez M., Leon G., Hidalgo A.M., Ruiz M.A., Phenol Removal from Water by Hybrid Processes: Study of the Membrane Process Step. *Desalination* **223**: 323–329 (2008).

[14] Hidalgo A.M., Leon G., Gomez M., Murcia M.D., Gomez E., Gomez J.L., Application of the Spiegler-Kedem-Kachalsky Model to the Removal of 4-Chlorophenol by Different Nanofiltration Membranes, *Desalination*, **315**: 70–75 (2013).

[15] Gomez J.L., Leon G., Hidalgo A.M., Gomez M., Murica M.D., Application of Reverse Osmosis to Remove Aniline from Wastewater, *Desalination*, **245**: 687-693 (2009).

[16] SKumar S, Malyan SK, Kumar A, NarsiR B., Optimization of Fenton's Oxidation by Box-Behnken Design of Response Surface Methodology for Landfill Leachate. *J. Mater. Environ. Sci.*, **7**(12): 4456–4466(2016).

[17] Moradi H., Sharifnia S., Rahimpour F., Photo Catalytic Decolorization of Reactive Yellow 84 from Aqueous Solutions Using ZnO Nanoparticles Supported on Mineral LECA, *Mater. Chem. Phys.*, **158**: 38-44 (2015).

[18] Shokri A., Mahanpoor K., Soodbar D., Evaluation of a Modified TiO_2 (GO–B–TiO_2) Photo Catalyst for Degradation of 4-Nitrophenol in Petrochemical Wastewater by Response Surface Methodology Based on the Central Composite Design, *J. Environ. Chem. Eng.*, **4**: 585–598 (2016).

[19] Shokri A., Rabiee F., Mahanpoor K., Employing a Novel Nano Catalyst (Mn/Iranian hematite) for Oxidation of SO_2 Pollutant in Aqueous Environment, *Int. J. Environ. Sci. Technol.*, **14**: 2485–2494 (2017).

[20] Kumar A., Prasad B., Mishra I.M., Optimization of Process Parameters for Acrylonitrile Removal by a Low-Cost Adsorbent Using Box-Behnken Design, *J. Hazard. Mater.*, **150**: 174–182(2008).

[21] Shokri A., Investigation of UV/H_2O_2 Process for Removal of Ortho-Toluidine from Industrial Wastewater by Response Surface Methodology Based on the Central Composite Design, *Desalin. Water Treat.*, **58**: 258–266(2017).

[22] Gullinkala T., Digman B., Gorey C., Hausman R., Escobar I.C., Chapter 4 Desalination: Reverse Osmosis and Membrane Distillation, *Sustainability Sci. Eng.*, **2**: 65–93(2010).

[23] Li Y., Wei J., Wang C., Wang W., Comparison of Phenol Removal in Synthetic Wastewater by NF or RO Membranes, *Desalin. Water Treat.*, **22**: 211–219 (2010).

[24] Simon A., Nghiem L.D., Le-Clech P., Khan S.J., Drewes J.E., Effects of Membrane Degradation on the Removal of Pharmaceutically Active Compounds (PhACs) by NF/RO Filtration Processes, *J. Membr. Sci.*, **340**: 16-25 (2009).

[25] Shokri A., Nasiri Shoja M., Employing Reverse Osmosis for the Removal of *ortho*-Toluidine from Wastewater, *Bulg. Chem. Commun.*, **50**: 21–26 (2018).

[26] Jaime Sadhwani Alonso J., El Kori N, Meli_an-Martel N., Del Rio-Gamero B., Removal of Ciprofloxacin from Seawater by Reverse Osmosis, *J. Environ. Manage.*, **217**: 337–345 (2018).